Available online at www.sciencedirect.com
SCIENCE DIRECT
Journal of Molecular Catalysis B: Enzymatic 38 (2006) 148–153
JOURNAL OF MOLECULAR CATALYSIS B: ENZYMATIC
www.elsevier.com/locate/molcatb

Study on the relationship between structure and enantioselectivity of a hyperthermophilic esterase from archaeon *Aeropyrum pernix* K1

Guirong Zhang [a,b], Renjun Gao [a], Liangyu Zheng [a], Aijun Zhang [a], Yuanhong Wang [a,c], Qiuyan Wang [a], Yan Feng [a], Shugui Cao [a,*]

[a] *Key Laboratory for Molecular Enzymology and Engineering of Ministry of Education, Jilin University, Changchun 130023, PR China*
[b] *Changchun Institute of Education, Changchun 130061, PR China*
[c] *Northeast Normal University, Changchun 130021, PR China*

Received 18 August 2005; received in revised form 20 October 2005; accepted 10 November 2005
Available online 30 January 2006

Abstract

To enhance the enantioselectivity of a hyperthermophilic esterase from archaeon *Aeropyrum pernix* K1 (APE1547), a directed evolution approach is employed to generate mutant library from the native enzyme. A mutation (TBC26) is identified after one round of epPCR. The enantioselectivity of TBC26 is increased up to 2.6-fold compared to that of wild type enzyme. TBC26 contains five amino acid substitutions (R11G, L36P, V223A, I551L, A564T). The five mutation sites are spatially distant to the catalytic center. According to the published crystal structure of WT and considering the changes of secondary and tertiary structure, here we try to explain the change of enantioselectivity of the TBC26. The results suggest that the change of enantioselectivity of enzyme has a close relationship to the configuration of the enzyme.

Keywords: Directed evolution; Enantioselectivity; Screening; 2-Octanol acetate; Configuration; Mutant

1. Introduction

Enantioselective enzymes, especially for those that catalyze hydrolysis reaction, are useful catalysts in production of pure enantiomers for pharmaceutical, agrochemical and bioactive materials [1]. Esterases are among the group of enzymes considered as potential catalysts in industrial process. Their enantioselectivity is one of the most important characteristics. With expanding applications of esterase in stereo-specific hydrolysis, transesterfication, and ester syntheses, its application in biotechnology is increasing rapidly.

Hyperthermophilic esterase from archaeon *Aeropyrum pernix* K1 has been shown to be one of the most thermostable esterase. Their activity is in the range of 50–90 °C [2]. The hyperthermophilic esterase with high enantioselectivity is more desirable for wide range of applications [3].

Directed evolution has been used to improve enantioselectivity for many enzymes [4]. In this study, the *rac*-2-octanol acetate which was a byproduct in our work was used as a substrate. In order to resolve the *rac*-2-octanol acetate, which was not accepted as substrate by the hyperthermophilic esterase (WT), a directed evolution of this esterase was performed. A major obstacle for this approach was lack of sensitive selection method because the hydrolysis reaction of this substrate could not be easily detected. The hydrolytic reaction of *rac*-2-octanol acetate was therefore monitored by pH indicator [5]. A mutant with higher enantioselectivity was selected from library of mutated enzymes. The relationship between *E*-value and structure of this enzyme was detected by Circular dichroism and Fluorescence spectroscopy. These results might facilitate further study of catalytic mechanism.

Abbreviations: BTB, bromothymol blue; APE1547, WT; Mutant enzyme, TBC26; epPCR, error-prone polymerase chain reaction

* Corresponding author. Tel.: +86 431 8924281; fax: +86 431 8987975.
E-mail address: sgcao@jlu.edu.cn (S. Cao).

1381-1177/$ – see front matter © 2005 Elsevier B.V. All rights reserved.
doi:10.1016/j.molcatb.2005.11.008

2. Materials and methods

2.1. Materials

Escherichia coli BL21 Codon-Plus (DE3) and vector pET15b were obtained from Novagen (Madison, WI). Taq DNA polymerase was purchased from New England Biolabs. Restriction enzymes were purchased from Promega and Toyobo (Osaka, Japan), ultrapure deoxynucleotide solution (dNTPs) was purchased from Pharmacia Biotech (Sweden). Isopryl-β-d-thiogalactopyranoside (IPTG), *p*-nitro-phenyl acetate (pNPC2) and *p*-nitro-phenyl caprylate (pNPC8) were purchased from Sigma. The *rac*-2-octanol acetate was synthesized by our lab.

2.2. Construction of the error-prone PCR mutant library

The gene APE1547 with lipase motif was chosen from the genome of *A. pernix* K1. The mutant library was obtained by epPCR. The epPCR was performed using upper primer: CTTACGAGTATCTCATATGCGCATTATAATGCCTGT (*Nde* I cutting site as underlined), lower primer: TTGGAGGCCCCTCCCGGCGGTGGATCCCTATCTCCT (*Bam* HI cutting site as underlined), 0.2 mM dNTP, Taq DNA polymerase and $MgCl_2$. The mutational rate was controlled by different concentration of $MgCl_2$. The epPCR program was 3 min at 94 °C, followed by 35 cycles of 1 min at 94 °C, 2 min at 48 °C, 3min at 72 °C, and finished by 10 min at 72 °C. The purification of the PCR product was inserted in pET 15b. The pET 15b was transformed to *E. coli* BL21 codon-plus (DE3) [2].

2.3. Initially screening system and expression of positive variants esterase

We used minimal media agar plate to screen the mutation library. The agar plate was supplemented with ampicillin (100 ug/ml), 0.1% (w/v) 2-octanol acetate, and had no the other carbon source. The agar plates were incubated at 37 °C.

A single-mutant (positive clone) was selected from the agar plate and inoculated to 96-well (A) plate. Positive clones were grown in 2YT medium (1% yeast extract, 1.6% tryptone, and 0.5% NaCl) containing ampicillin (100 ug/ml). After the 96-well (A) plate was incubated with shaking at 37 °C until the A_{600} reached 0.6–1.0, we transferred the single-mutant to another 96-well (B) plate used for obtaining the crude esterase. The 96-well (A) plate was stored at −20 °C, after adding 50% glycerol. The 96-well (B) plate was incubated with shaking at 37 °C until the A_{600} reached 0.6–1.0, the induction was carried out by adding IPTG at a final concentration of 1 mM and shaking for 4 h at 37 °C. The induced cells were collected by centrifugation and stored at −20 °C.

2.4. Purification of positive variants esterase

The positive variants esterase cells were frozen and melted three times, each time for 30 min. After the cells were mixed with 50 mM Tris–HCl buffer (pH 8.0),the cell suspension was centrifuged at 3000 rpm for 20 min. The supernatant was heated at 85 °C for 30 min. After centrifuging at 3000 rpm for 20 min at 4 °C, the supernatant was collected and the crude esterase was extracted.

2.5. Screening enantioselectivity of the variants library by PH-indicator

We used 96-well and pH-indicator (BTB) to screen the variants library. The reaction system includes pH-indicator (0.0016 mol/ml), phosphate buffer (20 mmol/L pH 7.3), crude esterase (300 U/ml) and *rac*-2-octaol acetate (0.01 v/v). The reaction was stopped when the color of reaction system changed to yellow. The wells were selected based on the color change from blue to yellow in 24 h.

2.6. Enzyme assay

The esterase from the positive variants was purified by Ni^{2+}-column pre-equilibrated with charge buffer (100 um $NiSO_4$, pH 8.0). The fractions were collected and the esterase activity was analyzed. The time course of the esterase-catalyzed hydrolysis of pNPC8 or pNPC2 was followed by monitoring the production of *p*-nitrophenyl at 405 nm in 1 cm path-length cells with a double-beam HTACHI 557 ultraviolet–visible spectrophotometer equipped with a temperature controller. The substrate pNPC8 or pNPC2 was dissolved in 10 mM acetonitrile [2]. For the standard assay, 20 ul of 10 mM pNPC8 or pNPC2 solution was added to 50 mM phosphate buffer (pH 8.0) in the reaction system incubated at 50 and 70 °C, respectively.

2.7. Gas chromatography (GC)

Enzymatic hydrolysis of *rac*-2-octanol acetate was monitored by GC. The reaction system was comprised of phosphate buffer solution (20 mM, pH 8.0); substrate (0.01 w/v) and the enzyme solution (300 U/ml). The conversion rate of substrate hydrolysis was determined by GC after 40 h. Shimadzu gas chromatograph (GC-14B) with a flame ionization detector at temperature programming between 110 and 210 °C was used to determine the concentration of 2-octanol [6]. (*S*)-2-octanol or (*R*)-2-octanol was derived from *R* (+)-1-phenylethyl isocyanate. The derivations were determined by gas chromatography after three hours (Fig. 1). The distinction of *R* from *S* enantiomers was achieved with temperature programming between 110 and 222 °C. The enantiomeric excess was determined by calculating the peak areas of two derivatives. The temperatures of the injector and the detector were 200 and 290 °C, respectively. Nitrogen was

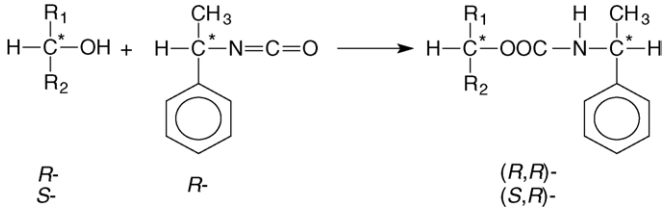

Fig. 1. (*S*)-2-octanol or (*R*)-2-octanol was derived from *R* (+)-1-phenylethyl isocyanate.

used as the carrier gas at a flow rate of 60 ml/min. The enantioselectivity of hydrolysis of *rac*-2-octanol acetate was calculated using the method of Chen et al. with $c = ee_s/(ee_s + ee_p)$ and $E = [\ln[1 - c(1 + ee_p)]/[\ln[1 - c]](1 - ee_p)]$ [7].

2.8. Circular dichroism

The circular dichroism (CD) spectra of APE1547 and TBC26 were measured by Jasco-810 spectropolarimeter (Japan). The enzyme (0.1 mg/ml) was incubated in phosphate buffer (20 mM, pH 8.0). CD measurement (200–300 nm) was done at 50 °C with a slit width of 1 nm. The kinetic process of ellipticity of the enzyme at 208 nm was recorded from 20 to 80 °C, using a solution containing protein (0.1 mg/ml) in phosphate buffer (20 mM, pH 8.0). The cell path length was 0.5 mm.

2.9. Fluorescence spectroscopy

Fluorescence spectra was recorded on a RF-5301Pc spectrofluorophotometer. The purified enzyme (0.1 mg/ml) was incubated in phosphate buffer (20 mM, pH 8.0) in a sealed optical cell for 20 min. Intrinsic fluorescence spectra of the recombinant enzyme at 300–400 nm were obtained with an excitation wavelength of 280 nm at 50 °C.

2.10. Molecular modeling

All computations were performed with InsightII package, version 2000 (Accelrys, San Diego, CA). The BIOPOLYMER module was used to create substrate molecular structures, energy minimizations were performed with the DISCOVER module using the consistent valence force field. The 1.8-Å crystallographic structure of APE1547 was used for the starting coordinates for calculations (Protein Data Bank, Brookhaven National Laboratory, code 1VE6 [PDB]). Hydrogen atoms were added at the normal ionization state of the amino acids at pH 7.0. The atomic potentials were fixed according to the consistent valence force field atom types recommended by the manufacture. Substrates were manually docked into the binding site of the enzymes, and was orientated with the oxyanion towards the oxyanion hole residues and the protonated N_ε of His_{act} embedded between the O_γ and the O_{ester} of the substrate. Residues contained in a simulation area within 15 Å from atom of N_ε of His_{act} were allowed to move with the remainder of the protein being fixed. A layer of 5 Å of explicit water was added to the surface of the assembly, and a nonbonded cutoff of 20 Å was fixed to reduce the time of calculation. Each structure was energy-minimized by applying 100 steps of steepest descents followed by a conjugate gradient minimization until convergence of 0.001 kcal mol^{-1} $Å^{-1}$.

3. Results and discussion

3.1. Construction and screening of the mutant library

The mutant library of the hyperthermophilic esterase from *A. pernix* K1 was constructed by ep-PCR. The vector pET15b connecting the mutant genes were transferred into the host *E. coli* BL21 Codon-Plus (DE3) and incubated overnight in minimal media agar plates with *rac*-2-octanol acetate as the only carbon source. The bacteria without genes of hyperthermophilis esterase could not grow on this plate. The WT colonies grow slower and smaller than the mutants on the plate. The mutants, with improved ability to metabolize *rac*-2-octanol acetate, form bigger and faster growing colonies were preferentially selected. The colony diameter of a positive mutant is more than 1 mm. When the mutant library was incubated overnight in 2YT agar plates; there were about 5000 colonies per plate. When the same mutant library was incubated overnight in minimal media agar plates with *rac*-2-octanol acetate as the only carbon source, there were only about 190 colonies per plate. This screening method increased the work efficiency about 26 folds.

Further selection was done by using pH indicator (BTB), according to the color change of the concentration of $[H]^+$ in the reaction process [8,9]. The enantioselectivity of hydrolysis was to compare the reactivity (in this case color change) of an enantiomer to the racemic mixture and thus estimate its enantioselectivity. For example, if the color of the racemic mixture changed much faster than that of the (*R*)-isomer, it was attributed to the faster hydrolysis of the (*S*)-isomer present in the racemic mixture, meaning the mutation was in favor of (*S*)-isomer. During in the reaction process, the color of the reaction system changed from blue to yellow.

Thirty-five variants with increasing enantioselectivity and activity for 2-octanol acetate were obtained by this screening (agar and pH indicator) methods. The enantioselectivity of esterase variant which hydrolyzed 2-octanol acetate was measured by GC (Fig. 2). We selected one of the best variant (TBC26) from mutant library. When TBC26 was with WT by sequences analysis, it was found that it contained five amino acid changes, namely: R11G, L36P, V223A, I551L and A564T.

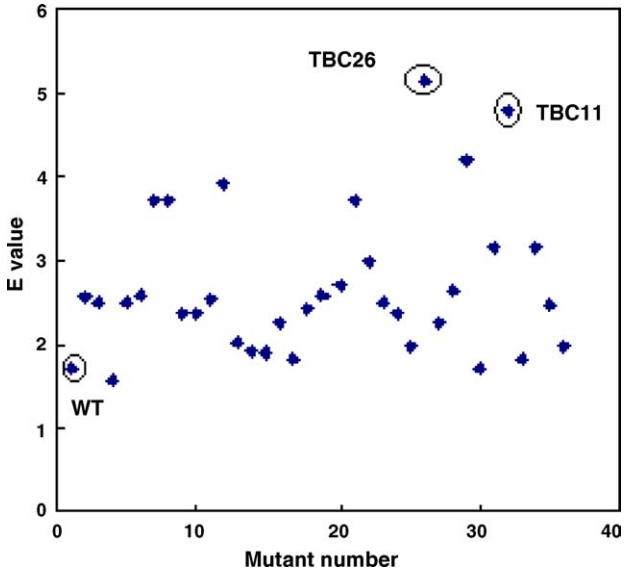

Fig. 2. Mutations were selected from mutant library. (⊙) TBC26 (R11G, L36P, V223A, I551L and A564T) and TBC11 (V1M, I20L, S42N, V92M).

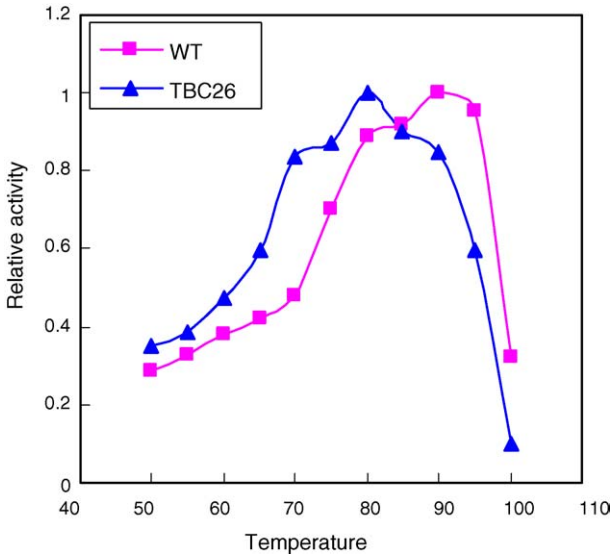

Fig. 3. Effect of temperature on activity of WT and TBC26.

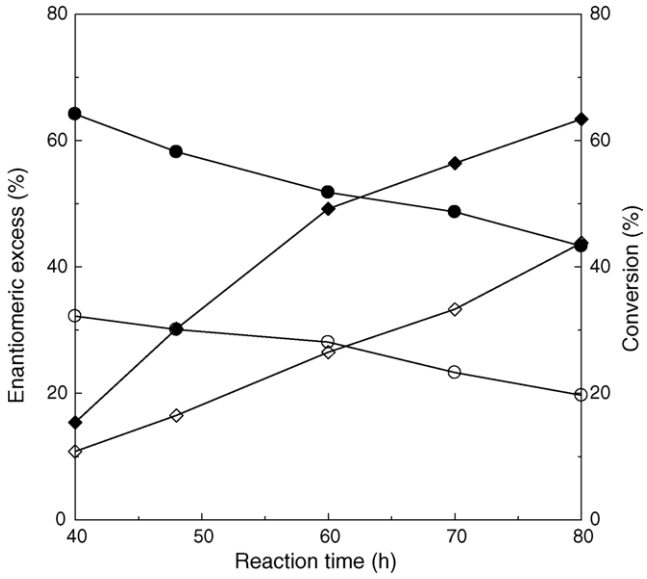

Fig. 4. Time course of hydrolyzed *rac*-2-octaol acetate at 50 °C. TBC26: (●) ee_p, (♦) conversion; WT: (○) ee_p, (◊) conversion. All assays were performed three times and average values were taken.

At 70 °C, the esterase activity of the TBC26 was 45% higher than that of WT (Fig. 3). The expression amount of TBC26 was 84% higher than that of WT.

3.2. Determination of enantioselectivity

The enantioselectivities of TBC26 and WT in the hydrolysis 2-octanol acetate were detected at 50 °C. The conversion ratios and ee_p of TBC26 were showed in Fig. 4. The *E*-value of TBC26 and WT hydrolyzed 2-octanol acetate were in favor of the (*S*)-enantiomer. The *E*-value of TBC26 was 2.6-fold that of WT. WT showed low enantioselectivity in favor of the (*S*)-enanomer at 50 °C.

3.3. Relationship between mutant site and E-value

According to the crystal structure, WT was composed of two domains, the β-propeller of N-terminal and α/β hydrolyase region at C-terminal. A short α-helix at the N-terminal (residues 8–23) extends from the β -propeller domain and forms part of the hydrolase domain [10]. The N-terminal was important for the catalytic activity. It connected with C-terminal structure region. If the N-terminal 1–22 amino acid were deleted, the stability of enzyme reduced and conformational flexibility of enzyme increased [11].

Comparing the selectivity of WT and TBC26, it showed that the *E*-value of TBC 26 was enhanced. The mutant site R11G was located within the N-terminal 1–22 amino acid residues. The Arg11 and Asp15 formed a hydrogen bond by the software of SPDBV. For the Gly substituted the Arg, the hydrogen bond was eliminated (Fig. 5). These affected the enzymic configuration and changed enantioselectivity [12,15].

If the 1–320 residues of WT were chopped off, the remaining segment would lose activity [11]. The sites L36P,V223A of the mutant TBC26 were located in this section. The enantiosecletivity of the mutant TBC26 had changed. The substitute might have

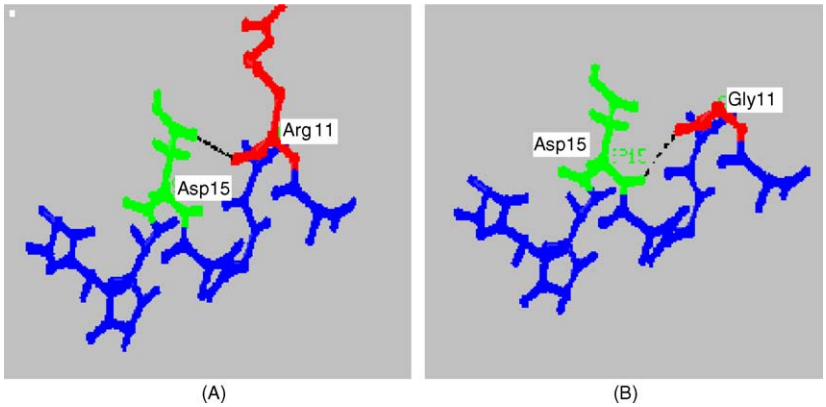

Fig. 5. (A) Crystal structure of WT showed the hydrogen bond between Arg11 and Asp15. (B) Crystal structure of TBC26 showed the hydrogen bond between Gly11 and Asp15.

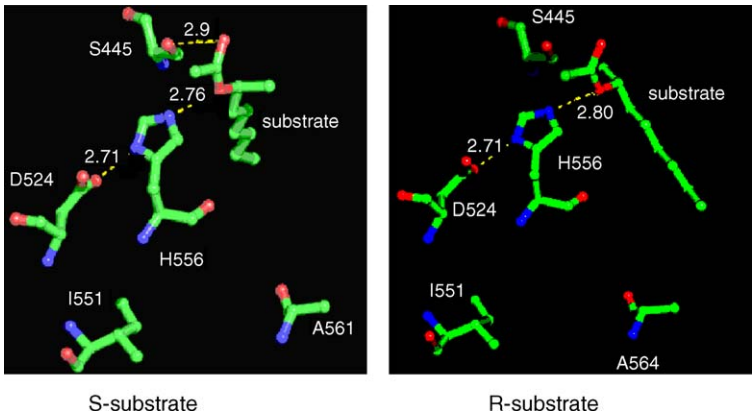

Fig. 6. After docking the substrate into the active site of the esterase *S*-2-octanol acetate and the Ser-445 formed a hydrogen bond, and *R*-2-octanol acetate and the Ser-445 did not form a hydrogen bond.

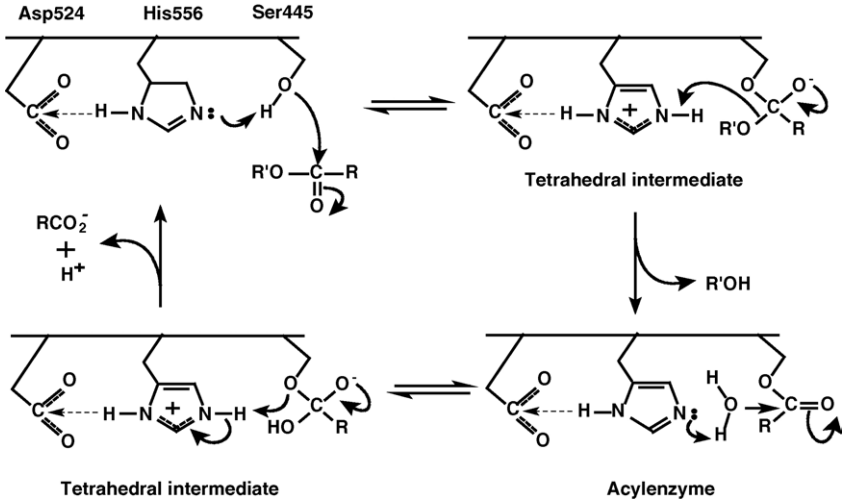

Fig. 7. Chemical mechanism of APE1547 analysis ester.

resulted in the change of the β-propeller and micro-environment in the catalytic reaction, and the Pro might caused β-sheet stop. These changes were likely to affect the enantiosecletivity of the enzyme.

It has been shown that Ser-445, Asp-524 and His-556 were located in the active site of WT and were required for the enzyme activity [10]. We had docked the substrate into the active site of the esterase. The s-substrate and the Ser-445 formed a hydrogen bond and the r-substrate could not form the hydrogen bond (Fig. 6). This accorded chemical mechanism of APE1547 analysis against ester (Fig. 7). The conformation of enzyme was in favor of (*S*)-substrate.

The mutant TBC26 of active sites was unchanged by detection sequence. The I551 of WT stood at 8.93, 7.12 and 9.12 Å to the active sites 556, 445 and substrate, respectively. Similarly, A564 was located at 9.49 and 7.37 Å to the active site 556 and substrate. After mutation the L551 of TBC26 stood at 6.71, 6.67 and 7.84 Å to the active sites 556, 445 and substrate, respectively. Similarly, T564 was located at 9.38 and 6.88 Å to the active site 556 and substrate (Fig. 8). From these results, we deduced that the increment of enantioselectivity resulted from the shorten of mutant distance.

It has been reported that the mutations far from the active site of enzyme might affect the enzymatic enantioselectivity [1,14,13].

3.4. Relationship of the structure and enantioselectivity

The *E*-value of TBC26 increased to 2.6-fold compared with that of WT. Furthermore, the structural changes of enzyme were detected by CD and fluorescence. We monitored WT and TBC26 before adding *rac*-2-octanol acetate by fluorescence spectra at 50 °C. In the reaction system, the λ_{max} of fluorescence was at 348 nm before adding substrate. The intrinsic fluorophores intensity of the TBC26 was higher than WT. The fluorescence intensity of the TBC26 at 348 and 303 nm was significantly higher than that of WT at 50 °C. These results suggested that the enzymatic enantioselectivity was relative to the intrinsic fluorescence value. The tryptophan and tyrosine residues led to the intrinsic fluorescence value. The hyperthermophilic esterase (WT) and mutant (TBC26) have the same tryptophan and tyrosine residues [9]. One of the possible reasons was that the change

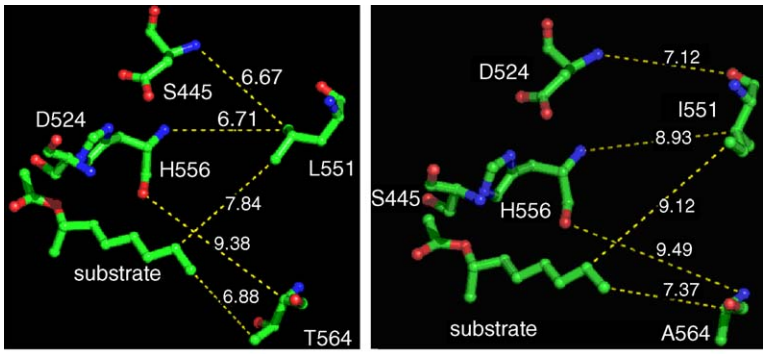

Fig. 8. The structure of WT contains three active sites (Ser-445, Asp-524 and His-556). The I551L and A564T amino acids are mutant residues. It showed the nearest distance of the I551L and A564T from active site and substrate, respectively.

Table 1
The change of *E*-value has a relationship with the content of α-helix, β-sheet, β-turn and random

Esterase	α-Helix	β-Sheet	β-Turn	Random
Wild-type	23.4	30.5	12.4	33.7
TBC26	26.5	27.2	12.2	34.0

of amino effect on the enzymeatic polarity and the alteration of the micro-environment of TBC26 caused the change of the enantioselectivity.

The result obtained from CD spectra during heat treatment showed a decrease in negative signals at wavelengths in the range 205 nm to 225 nm. The ellipticity of WT compared to TBC26 at 215 nm and 222 nm showed a remarkable decrease in negative signals. The *E*-value of TBC26 was 2.6-folds that of WT. Concerning the changes of the ellipticties of those related to α-helix and β-sheet (208, 215 and 222 nm), the data obtained suggest that the protein configuration including the secondary structure undergoes a structural rearrangement. These changes could be the cause of TBC26 tendency in favor of (*S*)-2-octanol acetate.

The CD data were calculated using the Jasco-810 spectropolarimeter software. The date show that the change of *E*-value is related with the content of α-helix, β-sheet, β-turn and random [10,15,16] (Table 1).

The changes of the fluorescence and CD showed that the tertiary structure of the enzymes (WT, TBC26) had significantly changed, compared to the secondary [17].

Based on the above analysis, it suggests that the *E*-value of the enzyme has relationship with conformational rigidity and flexibility of enzyme. In addition, it is possible that the enantioselectivity of the enzyme was correlated with microenvironment in catalytic reaction [18] and the mutations far from the active site may affect the enantioselectivity of enzyme. In summary, we had obtained the mutant that the enantioselectivity was enchanced by directed evolution. The reason for the change in enantioselectivity of the enzyme was analyzed based on structure. This showed relationship between structure and enantioselctivity.

Acknowledgements

The authors are grateful for the financial supports from the Natural Science Fund Program PR China (30400081, 30570405), the Key Technologies Research and Development Program PR China (2004BA713D03-04) and 973 Programmed of Ministry of Science and Technology, PR China (2004CB719606).

References

[1] G.P. Horsman, A.M.F. Liu, Henke, U.T. Bornscheuer, R.J. Kazlausks, Chem. Eur. J. 9 (2003) 1933–1939.
[2] R.J. Gao, Y. Feng, K. Ishikawa, H. Ishida, S. Ando, Y. Kosugi, S.G. Cao, J. Mol. Catal. B: Enzym. 24/25 (2003) 1–8.
[3] C. Yieille, G.J. Zeikus, Microbiol. Mol. Biol. Rev. Mar (2001) 1–43.
[4] B. Van Loo, J.H. Lutje Spelberg, J. Kingma, T. Sonke, M.G. Wubbolts, D.B. Janssen, Chem. Biol. 11 (2004) 981–990.
[5] L.E. Janes, A.C. Lowendahl, R.J. Kazlauskas, Chem. Eur. J. 4 (1998) 11.
[6] Z. Wang, Z.Q. Li, D.H. Yu, L. Weng, M. Liu, G.R. Zhang, S.G. Cao, Chem. Res. Chin. Univ. 20 (5) (2004) 575–578.
[7] C.S. Chen, Y. Fujimoto, G. Girdaukas, C.J. Sih, J. Am. Chem. Soc. 104 (1982) 7294–7299.
[8] U.T. Bornscheuer, J. Altenbuchner, H.H. Meyer, Bioorg. Med. Chem. 7 (1999) 2169–2173.
[9] F. Moris-Varas, A. Shah, J. Aikens, N.P. Nadkarni, D.J. Rozzell, D.C. Demirjian, Bioorg. Med. Chem. 7 (1999) 2183–2188.
[10] M. Bartlam, G.G. Wang, R.J. Gao, H. Yang, X. Zhao, G.Q. Xie, S.G. Cao, Y. Feng, Z.H. Rao, Structure 12 (2004) 1481–1488.
[11] B. Wang, Y. Feng, in press.
[12] K. Liebeton, A. Zonta, K. Schimossek, M. Nardini, D. Lang, B.W. Dijkstra, M.T. Reetz, K.-E. Jaeger, Chem. Biol. 7 (2000) 709–718.
[13] M.T. Reetz, K.-E. Jaeger, Chem. Eur. J. 6 (2000) 3.
[14] M.T. Reetz, C. Torre, A. Eipper, Org. Lett. 6 (2) (2004) 177–180.
[15] H.H.J. de Jongh, M.B.J. Meinders, Spectrochim. Acta Part A 58 (2002) 3197–3204.
[16] M. Bocola, N. Otte, K.-E. Jaeger, M.T. Reez, W. Thiel, ChemBioChem 5 (2004) 214–223.
[17] S.Y. Wang, Y. Feng, Arch. Biochem. Biophys. 411 (2003) 56–62.
[18] N.J. Greeneld, Trends Anal. Chem. 18 (1999) 4.